Responses to chronic corticosterone on brain glucocorticoid receptors, adrenal gland, and gut microbiota in mice lacking neuronal serotonin

Mariana Angoa-Pérez[a,b,*], **Branislava Zagorac**[a,b], **Dina M. Francescutti**[a,b], **Kevin R. Theis**[c,d], **Donald M. Kuhn**[a,b]

[a]Research and Development Service, John D. Dingell VA Medical Center, Detroit, MI, United States

[b]Department of Psychiatry and Behavioral Neurosciences, Wayne State University School of Medicine, Detroit, MI, United States

[c]Department of Biochemistry, Microbiology and Immunology, Wayne State University School of Medicine, Detroit, MI, United States

[d]Perinatal Research Initiative in Maternal, Perinatal and Child Health, Wayne State University School of Medicine, Detroit, MI, United States

Abstract

Dysregulation of the stress-induced activation of the hypothalamic-pituitary-adrenocortical axis can result in disease. Bidirectional communication exists between the brain and the gut, and alterations in these interactions appear to be involved in stress regulation and in the pathogenesis of neuropsychiatric diseases, such as depression. Serotonin (5HT) plays a crucial role in the functions of these two major organs but its direct influence under stress conditions remains unclear. To investigate the role of neuronal 5HT on chronic stress responses and its influence on the gut microbiome, mice lacking the gene for tryptophan hydroxylase-2 were treated with the stress hormone corticosterone (CORT) for 21 days. The intake of fluid and food, as well as body weights were recorded daily. CORT levels, expression of glucocorticoid receptors (GR) in the brain and the size of the adrenal gland were evaluated. Caecum was used for 16S rRNA gene characterization of the gut microbiota. Results show that 5HT depletion produced an increase in food intake and a paradoxical reduction in body weight that were enhanced by CORT. Neuronal 5HT depletion impaired the feedback regulation of CORT levels but had no putative effect on the

---

*Corresponding author at: Research and Development Service, John D. Dingell VA Medical Center, Detroit, MI, United States. maperez@med.wayne.edu (M. Angoa-Péerez).

CORT-induced decrease in hippocampal GR expression and the reduction of the adrenal cortex size. Finally, the composition and structure of the gut microbiota were significantly impacted by the absence of neuronal 5HT, and these alterations were enhanced by chronic CORT treatment. Therefore, we conclude that neuronal 5HT influences the stress-related responses at different levels involving CORT levels regulation and the gut microbiome.

Keywords

Tryptophan hydroxylase-2; Serotonin; Adrenal gland; Glucocorticoid receptor; Gut microbiota; 16S rRNA

1. Introduction

Stress activates the hypothalamic-pituitary-adrenocortical (HPA) axis and triggers the orchestration of neuroendocrine responses that enable the organisms to adapt to internal or external environment stimuli (Herman et al., 2016; Young et al., 2020; Zhang et al., 2017). The HPA axis mobilizes energy reserves through the release of glucocorticoids, to meet an organism's need for resources to cope with and adapt to stressors. Among the glucocorticoids (primarily cortisol in humans, corticosterone in rodents; hereafter referred to as CORT) released during stress, CORT is the main hormone released by the adrenal cortex and it serves as a master in the control of neuronal and signal transduction (Zhang et al., 2012). Proper regulation of the stress response is essential to avoid an energetically-costly HPA axis hyperactivity that could disrupt neuronal circuitries and result in disease (Herman et al., 2016; Wei et al., 2019). Monoamine neurotransmitters, particularly serotonin (5HT) are affected by stress (Favoretto et al., 2020), and it has been reported that functions of both the HPA axis and the 5HT system are commonly dysregulated in stress-related psychiatric disorders (Donner et al., 2016). For example, depression is associated with elevated basal glucocorticoid levels, dysfunctional negative feedback control of the HPA axis (Gillespie and Nemeroff 2005), and altered expression of 5HT effectors (Donner et al., 2016). While the mechanisms by which 5HT regulates stress responses in the brain are not completely understood, it has been found to be a key regulator of glucocorticoid receptor (GR) expression (Lai et al., 2003).

A bidirectional communication network exists between the brain and the gut, and the 5HT system plays a crucial role in the functions of these two major organs. Besides being a crucial transmitter in the brain, 5HT also regulates essential functions in the gut. In fact, about 95% of the body's 5HT is synthesized and stored in the gut (Banskota et al., 2019). While most of the enteric 5HT is synthesized in the enterochromaffin cells of the gastrointestinal mucosa through the tryptophan hydroxylase-1 isoform, the neuronal pool of 5HT is synthesized through the tryptophan hydroxylase-2 (TPH2) isoform and performs vital functions (Gross et al., 2012). Neuronal 5HT regulates sensory-motor and secretory actions in the gut, as well as motility and gastric emptying, and also appears to mediate proliferation and turnover of the intestinal mucosa (Gershon, 2013; Gross et al., 2012). Recently, it has become clear that the collection of microorganisms and their genomes in the intestinal habitat known as the gut microbiome, exerts control at multiple levels within

the body beyond the gastrointestinal tract (O'Mahony et al., 2015). While the number of microorganisms and host cells are of the same order of magnitude within the human body (Sender et al., 2016), the complex role of the gut microbiota within the brain-gut axis is just beginning to be elucidated. Nevertheless, it is already apparent that there is substantial overlap between the physiological relevance of the gut microbiota and the serotonergic system (O'Mahony et al., 2015). This is evidenced by the perturbations in the composition of the gut microbiota described in animal models of depression and chronic stress (Dinan and Cryan, 2013; Park et al., 2013). This link between the gut microbiota and depression is also evident in the alleviative effects of probiotic strains against psychological distress (Messaoudi et al., 2011), and in the utilization of antibacterial agents in the modulation of depression (Mello et al., 2013; Soczynska et al., 2012). Furthermore, recent preclinical studies demonstrated that transplantation of the gut microbiota from chronically stressed animals into healthy control mice was capable of inducing depression-like behaviors (Siopi et al., 2020). From a clinical perspective, understanding how interactions between neuronal 5HT and the gut microbiota affect stress responses could ultimately aid in the design of targeted treatments.

The CORT mouse model is widely used in preclinical research to further understanding of mechanisms of major depression (Demuyser et al., 2016). In this study, we used male mice devoid of neuronal 5HT to examine the stress responses induced by chronic administration of CORT on elements of the HPA axis and the gut microbiome. We have previously reported that these mice do not display a depression-like phenotype at baseline conditions, but they do develop this phenotype under chronic stress (Angoa-Perez et al., 2014).

2. Results

2.1. TPH2–/– mice displayed an increased intake of CORT and food, and a reduction in body weight that was aggravated by chronic CORT administration

The main effects of genotype ($F_{(3,34)} = 10.47$; $p < 0.0001$), time ($F_{(20,680)} = 3.84$; $p < 0.0001$), and the genotype X time interaction ($F_{(60,680)} = 3.02$; $p < 0.0001$) were significant for fluids intake (Fig. 1A). *Post hoc* comparisons indicate that in wild-type (WT) mice the intake of fluids with vehicle only did not differ from the intake of fluids with CORT. However, in TPH2–/– mice the intake of fluids with CORT was significantly higher than the intake of fluids with vehicle only ($p < 0.05$). While no significant genotype differences were observed in vehicle-drinking mice, the intake of fluids with CORT was higher in TPH2–/– mice than their WT counterparts ($p < 0.001$).

Similarly, there were significant effects of genotype ($F_{(3,26)} = 9.27$; $p < 0.002$), time ($F_{(20,520)} = 3.74$; $p < 0.0001$), and the genotype X time interaction ($F_{(60,520)} = 1.39$; $p < 0.03$) on food intake (Fig. 1B). Within each genotype, no differences in food intake were found when comparing mice drinking fluids with vehicle only to those receiving CORT. However, in vehicle-drinking mice, food intake was higher in TPH2–/– than in WT animals ($p < 0.05$). This genotype difference was also evident when comparing food intake in CORT-treated mice. TPH2–/– animals consumed significantly more food than their WT counterparts on CORT ($p < 0.01$).

The effects of genotype ($F_{(3,31)} = 15.21$; $p < 0.0001$), time ($F_{(20,620)} = 33.51$; $p < 0.0001$), and the genotype X time interaction ($F_{(60,620)} = 6.78$; $p < 0.0001$) were significant for body weight (Fig. 1C). While no differences were detected between vehicle-drinking WT mice compared to CORT animals of the same genotype, TPH2−/− mice receiving CORT weighed significantly less than TPH2−/− on vehicle ($p < 0.05$). Between genotypes, TPH2−/− mice drinking vehicle had a significantly lower body weight than WT mice on the same fluid ($p < 0.05$). CORT treatment resulted in lower body weight in TPH2−/− mice compared to WT animals ($p < 0.001$).

2.2. Levels of CORT in serum are decreased in TPH2−/− mice

Treatment with CORT had significant effects on the serum levels of this steroid ($F_{(1,21)} = 5.76$; $p < 0.05$; Fig. 2). While the effects of genotype were not significant, the treatment X genotype interaction was ($F_{(1,21)} = 11.91$; $p < 0.01$). CORT levels in mice receiving fluids with vehicle only indicated that basal levels of the steroid were higher in WT than in TPH2−/− mice ($p < 0.01$). CORT treatment induced a significant decrease in CORT serum levels in WT mice ($p < 0.01$) but not in TPH2−/− mice.

2.3. The decreased GR expression induced by chronic CORT administration was brain region-dependent

In the hippocampus dentate gyrus (DG), treatment with CORT had a significant effect ($F_{(1,24)} = 38.15$; $p < 0.0001$) on GR expression, whereas genotype and the interaction between genotype X treatment did not (Fig. 3A and 3D). While no differences between the two genotypes were present in the expression of GR in the DG, within each genotype the expression of these receptors was lower in CORT- than in vehicle-treated subjects ($p < 0.01$ for WT and $p < 0.001$ for TPH2−/− mice). GR expression in the CA1 area of the hippocampus did not show any significant effects of genotype or treatment (Fig. 3B and 3E). Although a tendency toward decreased expression of GR was evident in the hypothalamus of both WT and TPH2−/− mice treated with CORT versus vehicle-drinking TPH2−/− mice (Fig. 3C and 3F), this comparison did not reach statistical significance. There were no significant effects of treatment, genotype or their interaction in this brain area.

2.4. Chronic administration of CORT resulted in depression-like behaviors

The effects of genotype ($F_{(1,34)} = 8.85$; $p < 0.01$) and CORT treatment ($F_{(1,34)} = 38.91$; $p < 0.0001$) were significant for the splash test, whereas the interaction of genotype X treatment was not (Fig. 4). Within each genotype, the grooming time in this test was reduced after CORT treatment compared to the groups receiving vehicle ($p < 0.0001$ for WT mice; $p < 0.0001$ for TPH2−/− mice). There were no differences in grooming time between genotypes regardless of the treatment.

2.5. Chronic administration of CORT induced adrenal gland morphology and size alternations independent of neuronal 5HT

For measures of whole adrenal (Fig. 5A) and adrenal cortex size (Fig. 5B), only the effect of CORT treatment was significant ($F_{(1,24)} = 31.18$; $p < 0.0001$ for whole adrenal, $F_{(1,22)} = 38.56$; $p < 0.01$ for adrenal cortex); the effects of genotype and the interaction of genotype X

treatment were not. The size of the whole adrenal gland was reduced with CORT treatment in both genotypes compared to mice drinking vehicle only ($p < 0.5$ for WT and $p < 0.001$ for TPH2–/– mice).

Similarly, a reduction in adrenal cortex size was detected in CORT-treated WT ($p < 0.01$) and TPH2–/– ($p < 0.001$) mice compared to vehicle-treated controls.

2.6. TPH2–/– mice displayed gut microbiome alterations that were accentuated by chronic CORT administration

The mean ± SEM values of sequences were the following: 156,245 ± 14,309 in WT vehicle, 83,016 ± 7,544 in WT CORT, 123,301 ± 21,402 in TPH2–/– vehicle, and 69,410 ± 10,945 in TPH2–/– CORT. CORT administration resulted in a significantly lower sequences number in WT mice compared to their vehicle group ($p < 0.05$). To ensure that any observed differences in microbial diversity among treatment groups were not due to differential sequence depth and/or sample coverage, we subsampled each sample to 30,353 sequences, which was the lowest number of sequences obtained from any of the samples included in α-and β-diversity analyses. Average Good's coverage values for all treatment groups were at least 99.5%, and these values did not differ between CORT-treated and vehicle mice of each genotype.

A bimodal analysis of microbial biodiversity was employed by measuring both α- and β-diversity. Analyses of the α-diversity indices Chao-1 (Fig. 6A), reverse Simpson (Fig. 6B), and Shannon (Fig. 6C), did not reveal any significant differences between CORT- or vehicle-treated mice in either genotype.

Microbial β-diversity analyses revealed a significant effect of treatment ($F_{(1,17)} = 3.04$; $p < 0.0001$). The effects of genotype and the interaction between genotype X treatment were not significant. *Post hoc* comparisons for the Jaccard index indicate that WT mice receiving vehicle clustered separately from mice in the TPH2–/– vehicle group ($p < 0.05$). CORT treatment had a significant effect on the composition of gut microbial communities only in WT mice ($p < 0.01$), and there were no differences between CORT-treated mice when comparing the two genotypes (Fig. 7A). Analyses of the structure of the gut bacteria community with the Bray-Curtis index showed differences between the WT and TPH2–/– genotypes in vehicle-treated mice ($p < 0.05$). CORT treatment resulted in changes to the structure of gut microbial communities in both WT ($p < 0.05$) and TPH2–/– ($p < 0.05$) mice as compared to their corresponding vehicle-treated controls (Fig. 7B).

There was a significant effect of genotype on the relative abundance of the most prevalent bacteria phyla ($F_{(17,151} = 200$; $p < 0.0001$), as well as an effect of genotype X treatment interaction ($F_{(17,151)} = 4.12$; $p < 0.0001$). There was no significant effect of treatment (Fig. 8). For the Proteobacteria phylum, *post hoc* comparisons showed statistical differences only in the TPH2–/– genotype, with the vehicle-treated group displaying a lower relative abundance than the CORT-treated group ($p < 0.05$). For the Firmicutes phylum, the effects were significant only in WT mice, with an increase in the abundance of this phylum in the CORT-treated versus the vehicle-treated animals ($p < 0.01$). The last phylum displaying significant effects was Bacteroidetes, with decreases in its relative abundance with CORT

treatment in both WT (p < 0.0001) and THP2−/− (p < 0.001) genotypes compared to their corresponding genotype group receiving vehicle only (Fig. 8).

When the identities of the operational taxonomic units (OTUs, defined by clustering at 3% divergence and 97% similarity) with > 4% relative abundance were arrayed in a heat map for each subject from each group, the overall patterns are different within each genotype based on treatment and also between genotypes among mice treated equally (Fig. 9).

Linear discriminant analysis effect size (LEfSe) analyses show characteristic (i.e. discriminatory) OTUs for each of the four genotype-treatment groups (Fig. 10). Thus, these specific OTUs can be considered biomarkers of each condition. For WT mice receiving vehicle only, there were 4 characteristic OTUs that belonged to Prevotellacea, Bacteroides, *Helicobacter,* and Porphyromonadaceae, whereas Desulfovi-brionales was the only representative OTU of the WT CORT-treated mice. For the TPH2−/− mice receiving vehicle, there were 3 characteristic OTUs that included taxa within the Bacteroidetes phylum (Por-phyromonadaceae, Bacteroidetes and Bacteroidales), while Erysipelotrichaceae was the only OTU representative of the TPH2−/− CORT-treated mice (Fig. 10).

Finally, when the 16S rRNA gene sequences of OTUs with the highest relative abundances were taxonomically identified using the NCBI basic local alignment search tool (BLAST), four were matched to previously characterized bacterial species with > 99% sequence similarity (see Table 1). *Bacteroides acidifaciens* and *Helicobacter hepaticus* were identified in the WT vehicle-treated mice, *Lactobacillus reuteri* was identified in the TPH2−/− vehicle-treated group, and *Fecalibaculum rodentium* was identified in the TPH2−/− CORT-treated mice.

3. Discussion

The lack of neuronal 5HT had a clear effect on food intake and body weight in CORT-treated mice. While we did not observe differences in food intake or body weight in WT vehicle-treated compared to WT mice receiving CORT, the lack of 5HT was associated with a higher food intake and a paradoxical lower body weight in TPH2−/− mice (Fig. 1). It is well known that brain 5HT is a substantial regulator of food intake and appetite (D'Agostino et al., 2018). However, data on food intake and body weight in adult TPH2−/− mice shows discrepancies. While an early study found a decreased food intake in TPH2−/− mice (Yadav et al., 2009), a more recent report of these mice showed a tendency toward higher food intake and a significantly greater consumption of calories (van Lingen et al., 2019). This inconsistency could be explained by the gender of the mice and the methods used for measurement. The former report used pooled genders and single-day measurements from metabolic cage recordings, whereas the latter measured intake for several days and used only females. Our results agree with a higher food intake in TPH2−/− mice and are more comparable to the study of van Lingen et al., as we measured intake for 21 days. Although neither study reported body weight outcomes, a reduced body weight was reported in TPH2−/− females during the first 24 weeks of life and in TPH2−/− males throughout their lifespan (Lesch et al., 2012). Our results were consistent with this body weight reduction in TPH2−/− males and showed that CORT did not change these outcomes in food intake or

body weight. Interestingly, CORT intake was significantly increased only in TPH2−/− mice compared to the vehicle-treated group (Fig. 1).

Produced in the adrenal cortex, CORT is the major stress hormone in rodents that regulates stress-induced HPA axis activity (Mishima et al., 2015; Spiga and Lightman, 2015). There appears to be a consensus that chronic stress in rodent models results in increased levels of CORT (Karatsoreos et al., 2010; Ulrich-Lai et al., 2006). However, we observed higher baseline CORT levels in WT vehicle-treated compared to TPH2−/− vehicle-treated mice, and a decrease in this steroid in WT mice after repeated CORT administration (Fig. 2). We explain this outcome by a CORT-mediated negative feedback in WT mice. There is evidence that CORT can negatively regulate HPA axis activators such as the corticotropin-releasing hormone (CRH). Although we did not measure CRH levels, it is known that GR mediate this hormone actions and are highly expressed in hypothalamic CRH neurons (Gjerstad et al., 2018). Albeit not significant, expression of GR in the hypothalamus showed a tendency to a decrease and it was significantly reduced in the hippocampus (see Fig. 3). Early neuroanatomic evidence in rodents exists that hypothalamic 5HT-containing nerve terminals make direct input to CRH neurons to activate pituitary-adrenocortical secretion (Fuller 1996), and it has been shown that 5HT stimulates corticosteroid secretion in various species including humans (Contesse et al., 2000). These neuroanatomic findings support the pharmacologic evidence that activation of brain serotonergic function increases the release of CRH, adrenocorticotropic hormone and CORT. This is consistent with our findings of lower baseline CORT in serum of TPH2−/− mice, in which the lack the 5HT input for CORT release could explain the decrease in this steroid. Furthermore, it is important to emphasize that in addition to the baseline differences in CORT levels observed in the two genotypes, the regulation of CORT by neuronal 5HT was also evidenced by the blunted levels of this steroid after chronic stress in TPH2−/− mice.

Several findings suggest that CORT and GR are involved in the pathology of depression (Wang et al., 2019). The hippocampus is considered one of the most sensitive brain structures to stress, and in this area as well as in other brain regions, GR participate in adjusting responses to cope with stress through a negative feedback mechanism (McEwen 2007). Early postmortem analyses revealed that the levels of GR mRNA are decreased in the hippocampus of depressed suicidal patients (Modell et al., 1997). Our results show that GR expression in the DG was significantly decreased in both genotypes by chronic CORT administration (Fig. 3A). Early studies identified this subregion of the hippocampus as the neural substrate of the effects of GR activation on the adapted responses to stress (De Kloet et al., 1988). These results agree with studies showing that repeated stress reduced GR expression in the hippocampus (Gadek-Michalska et al., 2013), specifically in the DG and CA1 subregions of male rats (Kitraki et al., 2004). Although GR expression in the DG was robust, our conclusions for these receptors expression in other brain regions are limited by the small sample size analyzed. While GR expression in the CA1 subregion was also lower in CORT-treated mice of both genotypes, these changes were not statistically significant (Fig. 3B). These trends toward a decreased GR expression with CORT also apply to the hypothalamus (Fig. 3C), and although the reduction seems more accentuated in TPH2−/− mice, it still did not reach significance. The similarities in GR expression in WT and

TPH2−/− mice independent of the brain structure suggests that the depletion of brain 5HT does not have a major impact in the modulation of these receptors in those selected regions.

We have previously reported that TPH2−/− mice do not show a depression-like phenotype at baseline conditions, but they do develop this phenotype under chronic stress conditions (Angoa-Perez et al., 2014). The results from the chronic CORT administration in the current study confirm this notion and indicate there were no added effects evoked by the lack of neuronal 5HT as no genotype differences were found in the splash test (see Fig. 4).

The association between hyperactivity of the HPA axis and depression has been one of the most consistently reported findings in psychiatry (Juruena et al., 2018). Studies have looked at the morphology of effector organs, such as the adrenal glands to relate a possible HPA-dysregulation to organ function but the findings are heterogeneous (Kessing et al., 2011). While early evaluations of patients suffering from depression reported an enlargement of the adrenal gland (Rubin et al., 1996; Nemeroff et al., 1992), a more recent postmortem study identified no size differences in the adrenal region producing stress hormones in individuals with depressive disorder (Busch et al., 2020). Although preclinical studies have documented that chronic stress is associated with increases in adrenal weight (Kulkarni and Juvekar 2008) and hypertrophy (Ulrich-Lai et al., 2006), these changes seem to be specific to the sub-region of the adrenal cortex analyzed. While the zona glomerulosa experiences an increased cell density after stress, the inner zona fasciculata of the adrenal cortex and the medulla exhibited a decreased cell density (Ulrich-Lai et al., 2006). Moreover, other studies in rodents using a low and a high dose of CORT for 4 weeks reported decreases in weight of whole adrenals in both instances (Karatsoreos et al., 2010). Our results agree with those of Karatsoreos et al., as we clearly show a reduction in whole adrenal size and its cortex region, indicating that the effect of chronic CORT was associated with shrinkage rather than with hypertrophy (Fig. 5). This reduction in the adrenal cortex could explain the decreased levels of CORT measured in serum given that other studies have shown an association between the size of the adrenal with its production of CORT (Ulrich-Lai et al., 2006).

Clinical data have revealed that the gut microbiome is altered in patients with depression (Jiang et al., 2015), and preclinical studies also indicate that these intestinal bacteria are sensitive to the effects of depression (Dinan and Cryan, 2013; Partrick et al., 2018). To our knowledge, there are no published reports on gut microbiome status in the TPH2−/− mouse model. Data on the effects of chronic stress alone on α-diversity are variable. Reports using models with stressors over a time period similar to the one used in this study showed no differences in α-diversity measured by the Shannon index at the phylum level (Guo et al., 2019). Conversely, studies inflicting stress for a longer period (8 weeks), showed a lower Shannon index in the stress group versus controls (Siopi et al., 2020). Furthermore, measures of microbial richness (Chao-1 index) and α-diversity assessed by other indices such as Simpson and Shannon yielded no changes in mice subjected to chronic social defeat stress versus controls (Xie et al., 2020). Our results showed no differences in α-diversity in vehicle- or CORT-treated animals regardless of the genotype (Fig. 6). This suggests that the changes in α-diversity could emerge at lower taxonomic levels and after a more prolonged stress period. In terms of β-diversity, the lack of neuronal 5HT was associated with alterations in both the composition (Jaccard) and structure (Bray-Curtis) of the gut

bacteria communities (Fig. 7). There seems to be an agreement that chronic stress causes intestinal bacterial to cluster differently from controls regardless of the paradigm used (Gao et al., 2018; Siopi et al., 2020; Xie et al., 2020). Our results are consistent with this differential clustering in the principal coordinate analysis of WT vehicle-treated versus WT CORT-treated mice for both the composition and structure of the gut bacteria communities (Fig. 7). However, in TPH2−/− mice only the microbial community structure was changed by CORT, whereas the composition remained unaffected. These original findings are novel and add the modulation of the gut microbiome to the already ample repertoire of functions regulated by neuronal 5HT. At the level of bacterial phylum, chronic stress promoted a shift toward a reduction in Bacteroidetes and an increase in Firmicutes (Xie et al., 2019), two of the most prominent phyla in the intestines of mice and humans. We showed this shift to be true in WT mice but the relative abundance of Firmicutes in TPH2−/− mice treated with CORT, while higher than in TPH2−/− vehicle-treated subjects, did not reach statistical significance (Fig. 8). As observed in WT mice, the relative abundance of Bacteroidetes in TPH2−/− mice was lower with CORT treatment, suggesting that brain 5HT also influences the effects of stress on the gut bacteria composition. Interestingly, CORT administration increased the relative abundance of Proteobacteria only in TPH2−/− mice. Proteobacteria has been proposed as a microbial signature of gut dysbiosis, as its proliferation has been associated with increased risk of metabolic diseases (Shin et al., 2015). The exclusive increases in Proteobacteria in TPH2−/− subjects treated with CORT could be indicative of the role of neuronal 5HT as a protection factor against microbiota imbalances in stress conditions. All these 5HT- and stress-driven effects are evident in the heat map (Fig. 9), where the top 25 OTUs with relative abundances greater than 4% cluster separately based upon genotype and treatment.

LEfSe analyses revealed the presence of specific taxa that were more relatively abundant in one genotype-treatment group than in others. Thus, these microbial taxa could be considered bacterial biomarkers of each condition. These differences in taxa indicate basal genotype differences and also CORT-treatment effects specific to each genotype (Fig. 10). The WT vehicle-treated mice were characterized by taxa identified to the level of order, family and genus, with a majority of members from the phylum Bacteroidetes and one from Proteobacteria. The TPH2−/− vehicle-treated mice had representative taxa identified to the level of order, family and phylum with all 3 taxa from the phylum Bacteroidetes. The gut microbial communities of WT CORT-treated mice were characterized by bacteria in the order Desulfovibrionales, which belongs to the phylum Proteobacteria, while those of the TPH2−/− CORT-treated mice were characterized by bacteria in the family Erysi-pelotrichaceae, which belongs to the phylum Firmicutes.

Of the characteristic OTUs identified at the species level, *B. acidifaciens* was representative of the WT vehicle-treated group (Table 1). *B. acidifaciens* is a human commensal bacterium and it has been shown to be capable of preventing obesity and improving insulin sensitivity in mice (Yang et al., 2017). *H. hepaticus*, also present in the WT vehicle-treated group, has been found to colonize the lower intestine of mice without activating immune responses (Danne and Powrie 2018). While not strictly a commensal bacterium, *H. hepaticus* has the ability to induce anti-inflammatory responses in intestinal macrophages under host maladaptive events (Danne and Powrie 2018). Thus, it appears logical that these two

seemingly beneficial bacterial species were characteristic of the WT vehicle-treated group, which was not treated with CORT or lacked neuronal 5HT. Interestingly, *L. reuteri*, characteristic of the TPH2−/− vehicle-treated group, was effective in attenuating the depressive-like behaviors induced by chronic stress in mice through mechanisms involving 5HT regulation (Xie et al., 2020). Among the influence that *L. reuteri* exerted on the 5HT system were the increased the expression of its biosynthetic enzymes and the suppression of the tryptophan metabolism along the kynurenine pathway (Xie et al., 2020). While the expression of TPH2 could not be modulated by *L. reuteri* in constitutive TPH2−/− mice, the kynurenine pathway remains a possible target. Further studies are needed to corroborate this proposed effector but the characterization of *L. reuteri* as the representative bacterium in TPH2−/− mice supports its close association with the 5HT system. The TPH2−/− CORT treated mice were characterized by an increased abundance of *F. rodentium*, whose major metabolic end product is lactic acid (Zagato et al., 2020). It has been reported that accumulation of lactate in the colon has adverse effects on host health as high fecal lactate is associated with ulcerative colitis and bowel inflammation (Langille et al., 2014). Therefore, the increases in *F. rodentium* suggest the production of lactate as a factor mediating the effects of brain 5HT in the alterations produced by chronic stress.

While no gender differences in stress responses were found in previous studies with TPH2−/− mice, it is possible that the lack of neuronal 5HT could affect the composition of the gut microbiota differently in males and females. Studies have shown sex-related changes in the gut microbiome (Kim et al., 2020), and a modulation of metabolic functions by female hormones that is mediated by the gut microbiome (Kaliannan et al., 2018). Therefore, further studies in TPH2−/− females are needed to address these possibilities.

4. Conclusion

The results from the present study lead us to conclude that brain 5HT influences the effects chronic CORT at levels involving the HPA axis and the gut microbiome. Under basal conditions, TPH2−/− mice display a higher food intake and a paradoxical lower body weight that are aggravated by CORT. Although TPH2−/− mice do not exhibit depression-like behaviors under baseline circumstances, repeated administration of CORT resulted in a depressive-like phenotype. The feedback regulation of CORT levels under stress conditions was impaired in the absence of brain 5HT. However, the adrenal gland hypotrophy and the reduced adrenal cortex size induced by chronic CORT were not affected by the absence of central 5HT. Similarly, chronic CORT was associated with a reduced GR expression in the hippocampus DG and a tendency to lower levels in the hippocampus CA1 subregion and in the hypothalamus, all of which were not altered by the lack of neuronal 5HT. Finally, the composition and structure of the gut microbial community was significantly impacted in the absence of neuronal 5HT, and these alterations were enhanced by chronic CORT. More specifically, increases in Proteobacteria and members from Erysipelotrichaceae were exclusive of the combination of both CORT-induced stress and depletion of neuronal 5HT.

5. Experimental procedure

5.1. Subjects

Mice genetically modified to lack TPH2, the rate-limiting enzyme in the synthesis of brain 5HT, were generated on a C57BL/6 genetic background, as formerly described (Anneken et al., 2019; Thomas et al., 2010). Male TPH2−/− and WT littermates (8–14 weeks of age) were derived from heterozygous progenitors. Animals were individually housed in a room with monitored temperature and humidity and with alternating 12 h periods of light and darkness. No differences in stress responses of TPH2−/− mice were found by gender (Angoa-Perez et al., 2014), thus for this study only males were used. This study was carried out in strict accordance with the recommendations in the Guide for the Care and Use of Laboratory Animals of the National Institutes of Health. The protocol was approved by the Institutional Care and Use Committee of Wayne State University.

5.2. CORT administration

CORT was administered to individually housed TPH2−/− and WT mice in the drinking water for 21 days as previously described (Gasparini et al., 2016). Briefly, CORT powder (Sigma C2505) was first dissolved in 100% molecular grade ethanol and then added to the drinking water to the final concentration of 50 μg CORT/mL and 1% ethanol. Controls for each genotype received CORT vehicle in place of CORT. Each group contained the following sample sizes: WT vehicle n = 10, WT CORT n = 10, TPH2−/− vehicle n = 8, and TH2−/− CORT n = 10. Fresh solutions were prepared every other day and administered in graduated glass tubes (Braintree Scientific, Braintree, MA). Sipper tubes contained ball bearings to minimize loss of fluid to drippage. Mice had access to food and fluids *ad libitum*. Diet consisted of standard laboratory rodent chow (LabDiet 5001) containing 28.5% protein, 13.5% fat, and 58% carbohydrates. Intake of fluids and food as well as body weights were quantified daily throughout the treatment. Fluid intake was determined by weighing each bottle at the start of the test period and subtracting their weights after 24 h. Consumption for each mouse was normalized to body weight and presented as g of consumed food or fluid/g of body weight/24 h period. At the end of CORT administration, mice were sacrificed by decapitation and their brains were dissected for immunohistochemistry. In addition, serum samples were isolated from trunk blood to measure CORT levels using a high sensitivity ELISA (R & D Systems), and caecum samples collected for microbiome analyses. Samples were collected during the light phase between 09:00 and 11:00 am to avoid circadian variations of CORT.

5.3. Immunohistochemical analyses

Immunohistochemistry was performed as previously described (Briggs et al., 2016) with slight modifications. Coronal sections (30 μm) containing hippocampus and hypothalamus within the coordinates of bregma -1.355-mm and -1.955-mm were selected for analysis. Fixed sections were incubated with a rabbit monoclonal antibody against GR (D6H2L; Cell Signaling; 1:500) at 4 °C overnight. Primary antibody amplification was achieved using the Vectastain Elite ABC kit (Vector Labs, Burlingame, CA) according to the manufacturer's instructions. Sections were washed with PBS in between incubations. Diaminobenzidine staining solution (Vector Labs, Burlingame, CA) was added to each section for 5–10 min at

room temperature until sufficient color developed and the reaction was stopped with PBS. Sections were mounted on Fisher SuperFrost Plus Slides, dehydrated through graded ethanol washes, incubated in Citrisolv for 5 min, and coverslipped with Permount. Slides were allowed to dry overnight before viewing. Images were acquired at × 10 magnification using an Olympus BX51 microscope with a DP71 camera. Immunoreactivity was quantified with ImageJ software version 1.48v (NIH, Bethesda, MD; http://imagej.nih.gov/ij).

5.4. Splash test

To gauge motivational and self-care behavior, the splash test was performed as previously described (Angoa-Perez et al., 2014). In short, this test involves spraying a 10% sucrose solution onto the dorsal coat of a mouse in its home cage. This mildly sticky solution induces self-grooming the duration of which was recorded for 5 min by an observer blinded to mouse genotype. A reduced grooming time is considered a depression-like outcome.

5.5. Adrenal gland size and morphology

At the end of CORT administration, adrenal glands were removed bilaterally and fixed in 4% saline-buffered paraformaldehyde for at least 24 h. Fixed adrenal glands were cryoprotected in 30% sucrose for 48 h and frozen for sectioning. The entire adrenal gland was sectioned (30 μm) through its longest surface plane and the size of the whole adrenal was calculated by multiplying the total number of sections by the thickness. For measurement of the adrenal cortex, the largest section per adrenal was stained with hematoxylin and eosin (1 min each), dehydrated through graded ethanol washes, cleared with Citrisolv and coverslipped with Permount. Images at × 10 magnification were acquired using an Olympus BX51 fluorescence microscope with a DP71 camera. Cortices were measured longitudinally using the Olympus MicroSuite™ FIVE software for imaging applications.

5.6. Microbiome analysis

At the end of CORT administration, caecum contents were collected, immediately frozen in dry ice and stored at -80° C until further analysis. 16S rRNA genes in the caecum were sequenced as reported previously (Angoa-Perez et al., 2020). Briefly, bacterial DNA was extracted and purified using the QIAamp PowerFecal DNA Kit. The V4 hypervariable region of the bacterial 16S rRNA gene was amplified using dual indexed, Illumina compatible primers and the library was loaded onto an Illumina MiSeq standard V2 flow cell for sequencing in a 2x250bp paired end format. The 16S rRNA gene sequences from the paired fastq files were trimmed, screened and aligned using mothur (Schloss et al., 2009), in accordance with the MiSeq SOP protocol (https://www.mothur.org/wiki/MiSeq_SOP). Sequences were binned into OTUs defined by clustering at 3% divergence (97% similarity). Microbiome α-diversity was characterized using the Chao1 (i.e. community richness), Shannon and Simpson (1-D) (i.e. community heterogeneity) indices and the bacterial community data were thereafter visualized and statistically analyzed using PAST software (v3.20; (Hammer et al., 2001)). Microbial β-diversity was assessed using the Jaccard (i.e. shared composition) and Bray-Curtis (i.e. shared structure) indices based on OTU relative abundance data. High-dimensional class comparisons were carried out with linear discriminant analysis effect size (LEfSe) in an on-line interface (Afgan et al., 2018), using

default parameters with the exception that the LDA score was set to 3.6. Heat maps were generated using MetaboAnalyst 4.0 (Chong et al., 2018). All sequencing data were registered with the NCBI BioProject database and are publicly available under the ID: PRJNA666206.

5.7. Data analysis

CORT and food intake as well as body weight were analyzed with repeated-measures two-way ANOVA followed by Tukey's pairwise comparisons, using GraphPad Prism (v6.07) for Windows (GraphPad Software, La Jolla, CA, USA). The CORT ELISA, splash test, adrenal size and GR expression data were analyzed with two-way ANOVA followed by Tukey's multiple comparisons in Prism. Variation in the number of 16S rRNA gene sequences and Good's coverage values among murine genotype and treatment groups were analyzed with one-way ANOVA followed by Tukey's *post hoc* comparisons using Prism. The indices for α-diversity were obtained using PAST software (v 3.20), and statistically analyzed with two-way ANOVAs with Prism. The indices for β-diversity were both calculated and analyzed statistically with PAST using a two-way NPMANOVA (genotype X treatment). This analysis was followed by *post hoc* comparisons with one-way NPMANOVAs. Taxonomic distributions at the level of phylum were analyzed with a two-way ANOVA followed by Bonferroni's multiple comparisons tests, using Prism. LEfSe analyses were carried out using the Galaxy platform (Afgan et al., 2018) with default parameters (excluding using and LDA score of 3.6) and "all-against-all" comparisons.

Supplementary Material

Refer to Web version on PubMed Central for supplementary material.

Funding

References

Afgan E, Baker D, Batut B, van den Beek M, Bouvier D, Cech M, Chilton J, Clements D, Coraor N, Gruning BA, Guerler A, Hillman-Jackson J, Hiltemann S, Jalili V, Rasche H, Soranzo N, Goecks J, Taylor J, Nekrutenko A, Blankenberg D, 2018. The Galaxy platform for accessible, reproducible and collaborative biomedical analyses: 2018 update. Nucleic Acids Res. 46, W537–W544. 10.1093/nar/gky379. [PubMed: 29790989]

Angoa-Perez M, Kane MJ, Briggs DI, Herrera-Mundo N, Sykes CE, Francescutti DM, Kuhn DM, 2014. Mice genetically depleted of brain serotonin do not display a depression-like behavioral phenotype. ACS Chem. Neurosci. 5, 908–919. 10.1021/cn500096g. [PubMed: 25089765]

Angoa-Perez M, Zagorac B, Winters AD, Greenberg JM, Ahmad M, Theis KR, Kuhn DM, 2020. Differential effects of synthetic psychoactive cathinones and amphetamine stimulants on the gut microbiome in mice. PLoS ONE 15, e0227774. 10.1371/journal.pone.0227774. [PubMed: 31978078]

Anneken JH, Angoa-Perez M, Sati GC, Crich D, Kuhn DM, 2019. Dissociation between hypothermia and neurotoxicity caused by mephedrone and methcathinone in TPH2 knockout mice. Psychopharmacology 236, 1097–1106. 10.1007/s00213-018-4991-8. [PubMed: 30074064]

Banskota S, Ghia JE, Khan WI, 2019. Serotonin in the gut: blessing or a curse. Biochimie 161, 56–64. 10.1016/j.biochi.2018.06.008. [PubMed: 29909048]

Briggs DI, Angoa-Perez M, Kuhn DM, 2016. Prolonged repetitive head trauma induces a singular chronic traumatic encephalopathy-Like pathology in white matter despite transient behavioral abnormalities. Am. J. Pathol. 186, 2869–2886. 10.1016/j.ajpath.2016.07.013. [PubMed: 27662795]

Busch JR, Lundemose SB, Lynnerup N, Jacobsen C, Jorgensen MB, Banner J, 2020. Enlargement of the human adrenal zona fasciculata and chronic psychiatric illness - an autopsy-based study. Stress 23, 69–76. 10.1080/10253890.2019.1641485. [PubMed: 31322461]

Chong J, Soufan O, Li C, Caraus I, Li S, Bourque G, Wishart DS, Xia J, 2018. MetaboAnalyst 4.0: towards more transparent and integrative metabolomics analysis. Nucleic Acids Res. 46, W486–W494. 10.1093/nar/gky310. [PubMed: 29762782]

Contesse V, Lefebvre H, Lenglet S, Kuhn JM, Delarue C, Vaudry H, 2000. Role of 5-HT in the regulation of the brain-pituitary-adrenal axis: effects of 5-HT on adrenocortical cells. Can. J. Physiol. Pharmacol. 78, 967–983.

D'Agostino G, Lyons D, Cristiano C, Lettieri M, Olarte-Sanchez C, Burke LK, Greenwald-Yarnell M, Cansell C, Doslikova B, Georgescu T, Martinez de Morentin PB, Myers MG Jr., Rochford JJ, Heisler LK, 2018. Nucleus of the solitary tract serotonin 5-HT2C receptors modulate food intake. Cell Metab. 28, 619–630.e615. 10.1016/j.cmet.2018.07.017. [PubMed: 30146485]

Danne C, Powrie F, 2018. Helicobacter hepaticus polysaccharide induces an anti-inflammatory response in intestinal macrophages. Microb. Cell 5, 208–211. 10.15698/mic2018.04.626. [PubMed: 29611556]

De Kloet ER, De Kock S, Schild V, Veldhuis HD, 1988. Antiglucocorticoid RU 38486 attenuates retention of a behaviour and disinhibits the hypothalamic-pituitary adrenal axis at different brain sites. Neuroendocrinology 47, 109–115. 10.1159/000124900. [PubMed: 3344063]

Demuyser T, Bentea E, Deneyer L, Albertini G, Massie A, Smolders I, 2016. Disruption of the HPA-axis through corticosterone-release pellets induces robust depressive-like behavior and reduced BDNF levels in mice. Neurosci. Lett. 626, 119–125. 10.1016/j.neulet.2016.05.026. [PubMed: 27208833]

Dinan TG, Cryan JF, 2013. Melancholic microbes: a link between gut microbiota and depression? Neurogastroenterol. Motil 25, 713–719. 10.1111/nmo.12198. [PubMed: 23910373]

Donner NC, Siebler PH, Johnson DT, Villarreal MD, Mani S, Matti AJ, Lowry CA, 2016. Serotonergic systems in the balance: CRHR1 and CRHR2 differentially control stress-induced serotonin synthesis. Psychoneuroendocrinology 63, 178–190. 10.1016/j.psyneuen.2015.09.024. [PubMed: 26454419]

Favoretto CA, Nunes YC, Macedo GC, Lopes JSR, Quadros IMH, 2020. Chronic social defeat stress: impacts on ethanol-induced stimulation, corticosterone response, and brain monoamine levels. J. Psychopharmacol. 34, 412–419. 10.1177/0269881119900983. [PubMed: 31965898]

Fuller RW, 1996. Serotonin receptors involved in regulation of pituitary-adrenocortical function in rats. Behav. Brain Res. 73, 215–219. 10.1016/0166-4328(96)00099-x. [PubMed: 8788505]

Gadek-Michalska A, Spyrka J, Rachwalska P, Tadeusz J, Bugajski J, 2013. Influence of chronic stress on brain corticosteroid receptors and HPA axis activity. Pharmacol. Rep. 65, 1163–1175. 10.1016/s1734-1140(13)71474-9. [PubMed: 24399712]

Gao X, Cao Q, Cheng Y, Zhao D, Wang Z, Yang H, Wu Q, You L, Wang Y, Lin Y, Li X, Wang Y, Bian JS, Sun D, Kong L, Birnbaumer L, Yang Y, 2018. Chronic stress promotes colitis by disturbing the gut microbiota and triggering immune system response. Proc. Natl. Acad. Sci. U.S.A. 115, E2960–E2969. 10.1073/pnas.1720696115. [PubMed: 29531080]

Gasparini SJ, Weber MC, Henneicke H, Kim S, Zhou H, Seibel MJ, 2016. Continuous corticosterone delivery via the drinking water or pellet implantation: a comparative study in mice. Steroids 116, 76–82. 10.1016/j.steroids.2016.10.008. [PubMed: 27815034]

Gershon MD, 2013. 5-Hydroxytryptamine (serotonin) in the gastrointestinal tract. Curr. Opin. Endocrinol. Diabetes Obes. 20, 14–21. 10.1097/MED.0b013e32835bc703. [PubMed: 23222853]

Gillespie CF, Nemeroff CB, 2005. Hypercortisolemia and depression. Psychosom. Med. 67 (Suppl 1), S26–S28. 10.1097/01.psy.0000163456.22154.d2. [PubMed: 15953796]

Gjerstad JK, Lightman SL, Spiga F, 2018. Role of glucocorticoid negative feedback in the regulation of HPA axis pulsatility. Stress 21, 403–416. 10.1080/10253890.2018.1470238. [PubMed: 29764284]

Gross ER, Gershon MD, Margolis KG, Gertsberg ZV, Li Z, Cowles RA, 2012. Neuronal serotonin regulates growth of the intestinal mucosa in mice. Gastroenterology 143, 408–417.e402. 10.1053/j.gastro.2012.05.007. [PubMed: 22609381]

Guo Y, Xie JP, Deng K, Li X, Yuan Y, Xuan Q, Xie J, He XM, Wang Q, Li JJ, Luo HR, 2019. Prophylactic effects of Bifidobacterium adolescentis on anxiety and depression-like phenotypes after chronic stress: a role of the gut microbiota-inflammation axis. Front. Behav. Neurosci. 13, 126. 10.3389/fnbeh.2019.00126. [PubMed: 31275120]

Hammer O, Harper DAT, Ryan PD, 2001. PAST: paleontological statistics software package for education and data analysis. Palaeontologia Electonica 4, 1–9.

Herman JP, McKlveen JM, Ghosal S, Kopp B, Wulsin A, Makinson R, Scheimann J, Myers B, 2016. Regulation of the hypothalamic-pituitary-adrenocortical stress response. Compr. Physiol. 6, 603–621. 10.1002/cphy.c150015. [PubMed: 27065163]

Jiang H, Ling Z, Zhang Y, Mao H, Ma Z, Yin Y, Wang W, Tang W, Tan Z, Shi J, Li L, Ruan B, 2015. Altered fecal microbiota composition in patients with major depressive disorder. Brain Behav. Immun. 48, 186–194. 10.1016/j.bbi.2015.03.016. [PubMed: 25882912]

Juruena MF, Bocharova M, Agustini B, Young AH, 2018. Atypical depression and non-atypical depression: Is HPA axis function a biomarker? A systematic review. J. Affect Disord. 233, 45–67. 10.1016/j.jad.2017.09.052. [PubMed: 29150144]

Kaliannan K, Robertson RC, Murphy K, Stanton C, Kang C, Wang B, Hao L, Bhan AK, Kang JX, 2018. Estrogen-mediated gut microbiome alterations influence sexual dimorphism in metabolic syndrome in mice. Microbiome 6, 205. 10.1186/s40168-018-0587-0. [PubMed: 30424806]

Karatsoreos IN, Bhagat SM, Bowles NP, Weil ZM, Pfaff DW, McEwen BS, 2010. Endocrine and physiological changes in response to chronic corticosterone: a potential model of the metabolic syndrome in mouse. Endocrinology 151, 2117–2127. 10.1210/en.2009-1436. [PubMed: 20211972]

Kessing LV, Willer IS, Knorr U, 2011. Volume of the adrenal and pituitary glands in depression. Psychoneuroendocrinology 36, 19–27. 10.1016/j.psyneuen.2010.05.007. [PubMed: 20646833]

Kim YS, Unno T, Kim BY, Park MS, 2020. Sex differences in gut microbiota. World J. Mens. Health 38, 48–60. 10.5534/wjmh.190009. [PubMed: 30929328]

Kitraki E, Kremmyda O, Youlatos D, Alexis MN, Kittas C, 2004. Gender-dependent alterations in corticosteroid receptor status and spatial performance following 21 days of restraint stress. Neuroscience 125, 47–55. 10.1016/j.neuroscience.2003.12.024. [PubMed: 15051144]

Kulkarni MP, Juvekar AR, 2008. Attenuation of acute and chronic restraint stress-induced perturbations in experimental animals by Nelumbo nucifera gaertn. Indian J. Pharm. Sci. 70, 327–332. 10.4103/0250-474x.42982. [PubMed: 20046740]

Lai M, McCormick JA, Chapman KE, Kelly PA, Seckl JR, Yau JL, 2003. Differential regulation of corticosteroid receptors by monoamine neurotransmitters and antidepressant drugs in primary hippocampal culture. Neuroscience 118, 975–984. 10.1016/s0306-4522(03)00038-1. [PubMed: 12732243]

Langille MG, Meehan CJ, Koenig JE, Dhanani AS, Rose RA, Howlett SE, Beiko RG, 2014. Microbial shifts in the aging mouse gut. Microbiome 2, 50. 10.1186/s40168-014-0050-9. [PubMed: 25520805]

Lesch KP, Araragi N, Waider J, van den Hove D, Gutknecht L, 2012. Targeting brain serotonin synthesis: insights into neurodevelopmental disorders with long-term outcomes related to negative emotionality, aggression and antisocial behaviour. Philos. Trans. R. Soc. Lond. B Biol. Sci. 367, 2426–2443. 10.1098/rstb.2012.0039. [PubMed: 22826343]

McEwen BS, 2007. Physiology and neurobiology of stress and adaptation: central role of the brain. Physiol. Rev. 87, 873–904. 10.1152/physrev.00041.2006. [PubMed: 17615391]

Mello BS, Monte AS, McIntyre RS, Soczynska JK, Custodio CS, Cordeiro RC, Chaves JH, Vasconcelos SM, Nobre HV Jr., Florenco de Sousa FC, Hyphantis TN, Carvalho AF, Macedo DS, 2013. Effects of doxycycline on depressive-like behavior in mice after lipopolysaccharide (LPS) administration. J. Psychiatr. Res. 47, 1521–1529. 10.1016/j.jpsychires.2013.06.008. [PubMed: 23835040]

Messaoudi M, Lalonde R, Violle N, Javelot H, Desor D, Nejdi A, Bisson JF, Rougeot C, Pichelin M, Cazaubiel M, Cazaubiel JM, 2011. Assessment of psychotropic-like properties of a probiotic

formulation (Lactobacillus helveticus R0052 and Bifidobacterium longum R0175) in rats and human subjects. Br. J. Nutr. 105, 755–764. 10.1017/s0007114510004319. [PubMed: 20974015]

Mishima Y, Shinoda Y, Sadakata T, Kojima M, Wakana S, Furuichi T, 2015. Lack of stress responses to long-term effects of corticosterone in Caps2 knockout mice. Sci. Rep. 5, 8932. 10.1038/srep08932. [PubMed: 25754523]

Modell S, Yassouridis A, Huber J, Holsboer F, 1997. Corticosteroid receptor function is decreased in depressed patients. Neuroendocrinology 65, 216–222. https://doi. org/10.1159/000127275. [PubMed: 9088003]

Nemeroff CB, Krishnan KR, Reed D, Leder R, Beam C, Dunnick NR, 1992. Adrenal gland enlargement in major depression. A computed tomographic study. Arch. Gen. Psychiatry 49, 384–387. 10.1001/archpsyc.1992.01820050048008. [PubMed: 1586274]

O'Mahony SM, Clarke G, Borre YE, Dinan TG, Cryan JF, 2015. Serotonin, tryptophan metabolism and the brain-gut-microbiome axis. Behav. Brain Res. 277, 32–48. 10.1016/j.bbr.2014.07.027. [PubMed: 25078296]

Park AJ, Collins J, Blennerhassett PA, Ghia JE, Verdu EF, Bercik P, Collins SM, 2013. Altered colonic function and microbiota profile in a mouse model of chronic depression. Neurogastroenterol. Motil. 25, 733–e575. 10.1111/nmo.12153. [PubMed: 23773726]

Partrick KA, Chassaing B, Beach LQ, McCann KE, Gewirtz AT, Huhman KL, 2018. Acute and repeated exposure to social stress reduces gut microbiota diversity in Syrian hamsters. Behav. Brain Res. 345, 39–48. 10.1016/j.bbr.2018.02.005. [PubMed: 29474810]

Rubin RT, Phillips JJ, McCracken JT, Sadow TF, 1996. Adrenal gland volume in major depression: relationship to basal and stimulated pituitary-adrenal cortical axis function. Biol. Psychiatry 40, 89–97. 10.1016/0006-3223(95)00358-4. [PubMed: 8793041]

Schloss PD, Westcott SL, Ryabin T, Hall JR, Hartmann M, Hollister EB, Lesniewski RA, Oakley BB, Parks DH, Robinson CJ, Sahl JW, Stres B, Thallinger GG, Van Horn DJ, Weber CF, 2009. Introducing mothur: open-source, platform-independent, community-supported software for describing and comparing microbial communities. Appl. Environ. Microbiol. 75, 7537–7541. 10.1128/aem.01541-09. [PubMed: 19801464]

Sender R, Fuchs S, Milo R, 2016. Revised estimates for the number of human and bacteria cells in the body. PLoS Biol. 14, e1002533 10.1371/journal.pbio.1002533. [PubMed: 27541692]

Shin NR, Whon TW, Bae JW, 2015. Proteobacteria: microbial signature of dysbiosis in gut microbiota. Trends Biotechnol. 33, 496–503. 10.1016/j.tibtech.2015.06.011. [PubMed: 26210164]

Siopi E, Chevalier G, Katsimpardi L, Saha S, Bigot M, Moigneu C, Eberl G, Lledo PM, 2020. Changes in gut microbiota by chronic stress impair the efficacy of fluoxetine. Cell Rep. 30, 3682–3690.e3686. 10.1016/j.celrep.2020.02.099. [PubMed: 32187541]

Soczynska JK, Mansur RB, Brietzke E, Swardfager W, Kennedy SH, Woldeyohannes HO, Powell AM, Manierka MS, McIntyre RS, 2012. Novel therapeutic targets in depression: minocycline as a candidate treatment. Behav. Brain Res. 235, 302–317. 10.1016/j.bbr.2012.07.026. [PubMed: 22963995]

Spiga F, Lightman SL, 2015. Dynamics of adrenal glucocorticoid steroidogenesis in health and disease. Mol. Cell. Endocrinol. 408, 227–234. 10.1016/j.mce.2015.02.005. [PubMed: 25662280]

Thomas DM, Angoa Perez M, Francescutti-Verbeem DM, Shah MM, Kuhn DM, 2010. The role of endogenous serotonin in methamphetamine-induced neurotoxicity to dopamine nerve endings of the striatum. J. Neurochem. 115, 595–605. 10.1111/j.1471-4159.2010.06950.x. [PubMed: 20722968]

Ulrich-Lai YM, Figueiredo HF, Ostrander MM, Choi DC, Engeland WC, Herman JP, 2006. Chronic stress induces adrenal hyperplasia and hypertrophy in a subregion-specific manner. Am. J. Physiol. Endocrinol. Metab 291, E965–E973. 10.1152/ajpendo.00070.2006. [PubMed: 16772325]

van Lingen M, Sidorova M, Alenina N, Klempin F, 2019. Lack of brain serotonin affects feeding and differentiation of newborn cells in the adult hypothalamus. Front. Cell Dev. Biol. 7, 65. 10.3389/fcell.2019.00065. [PubMed: 31106202]

Wang W, Liu L, Yang X, Gao H, Tang QK, Yin LY, Yin XY, Hao JR, Geng DQ, Gao C, 2019. Ketamine improved depressive-like behaviors via hippocampal glucocorticoid receptor in chronic

stress induced- susceptible mice. Behav. Brain Res. 364, 75–84. 10.1016/j.bbr.2019.01.057. [PubMed: 30753876]

Wei CL, Wang S, Yen JT, Cheng YF, Liao CL, Hsu CC, Wu CC, Tsai YC, 2019. Antidepressant-like activities of live and heat-killed Lactobacillus paracasei PS23 in chronic corticosterone-treated mice and possible mechanisms. Brain Res. 1711, 202–213. 10.1016/j.brainres.2019.01.025. [PubMed: 30684456]

Xie R, Jiang P, Lin L, Jiang J, Yu B, Rao J, Liu H, Wei W, Qiao Y, 2020. Oral treatment with Lactobacillus reuteri attenuates depressive-like behaviors and serotonin metabolism alterations induced by chronic social defeat stress. J. Psychiatr. Res. 122, 70–78. 10.1016/j.jpsychires.2019.12.013. [PubMed: 31927268]

Xie X, Xiao Q, Xiong Z, Yu C, Zhou J, Fu Z, 2019. Crocin-I ameliorates the disruption of lipid metabolism and dysbiosis of the gut microbiota induced by chronic corticosterone in mice. Food Funct. 10, 6779–6791. 10.1039/c9fo01533g. [PubMed: 31576875]

Yadav VK, Oury F, Suda N, Liu ZW, Gao XB, Confavreux C, Klemenhagen KC, Tanaka KF, Gingrich JA, Guo XE, Tecott LH, Mann JJ, Hen R, Horvath TL, Karsenty G, 2009. A serotonin-dependent mechanism explains the leptin regulation of bone mass, appetite, and energy expenditure. Cell 138, 976–989. 10.1016/j.cell.2009.06.051. [PubMed: 19737523]

Yang JY, Lee YS, Kim Y, Lee SH, Ryu S, Fukuda S, Hase K, Yang CS, Lim HS, Kim MS, Kim HM, Ahn SH, Kwon BE, Ko HJ, Kweon MN, 2017. Gut commensal Bacteroides acidifaciens prevents obesity and improves insulin sensitivity in mice. Mucosal Immunol. 10, 104–116. 10.1038/mi.2016.42. [PubMed: 27118489]

Young ES, Doom JR, Farrell AK, Carlson EA, Englund MM, Miller GE, Gunnar MR, Roisman GI, Simpson JA, 2020. Life stress and cortisol reactivity: An exploratory analysis of the effects of stress exposure across life on HPA-axis functioning. Dev. Psychopathol 1–12 10.1017/s0954579419001779.

Zagato E, Pozzi C, Bertocchi A, Schioppa T, Saccheri F, Guglietta S, Fosso B, Melocchi L, Nizzoli G, Troisi J, Marzano M, Oresta B, Spadoni I, Atarashi K, Carloni S, Arioli S, Fornasa G, Asnicar F, Segata N, Guglielmetti S, Honda K, Pesole G, Vermi W, Penna G, Rescigno M, 2020. Endogenous murine microbiota member Faecalibaculum rodentium and its human homologue protect from intestinal tumour growth. Nat. Microbiol. 5, 511–524. 10.1038/s41564-019-0649-5. [PubMed: 31988379]

Zhang J, Fan Y, Li Y, Zhu H, Wang L, Zhu MY, 2012. Chronic social defeat up-regulates expression of the serotonin transporter in rat dorsal raphe nucleus and projection regions in a glucocorticoid-dependent manner. J. Neurochem. 123, 1054–1068. 10.1111/jnc.12055. [PubMed: 23061525]

Zhang J, Fan Y, Raza MU, Zhan Y, Du XD, Patel PD, Zhu MY, 2017. The regulation of corticosteroid receptors in response to chronic social defeat. Neurochem. Int. 108, 397–409. 10.1016/j.neuint.2017.05.021. [PubMed: 28577990]
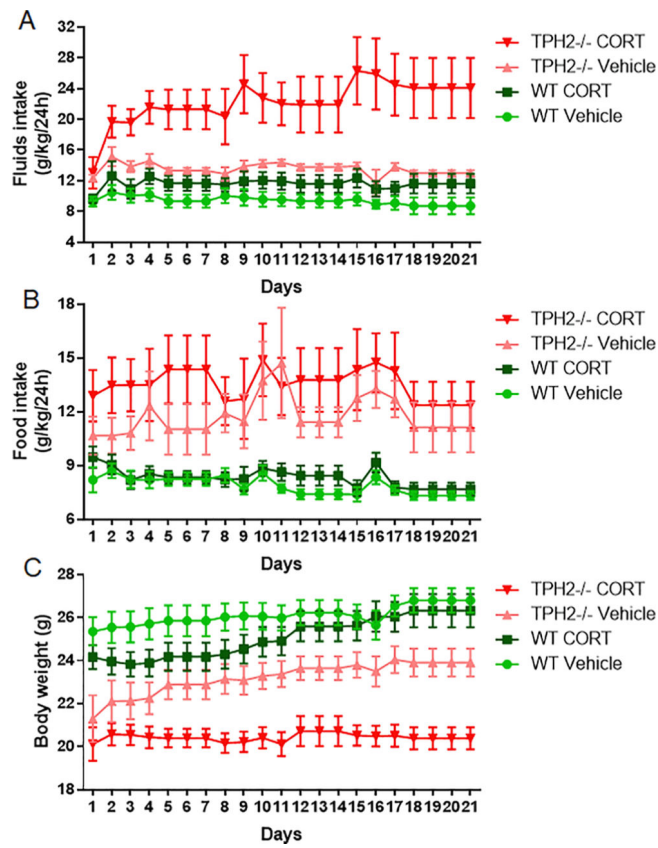
Fig. 1.
Fluids intake (A), food intake (B) and body weight (C) in WT (n = 8–10) and TPH2–/– (n = 6–9) mice treated with corticosterone (CORT) or vehicle over 21 days. Intakes are shown in g of consumed fluids or food/g of body weight/24 h. Mean ± SEM.
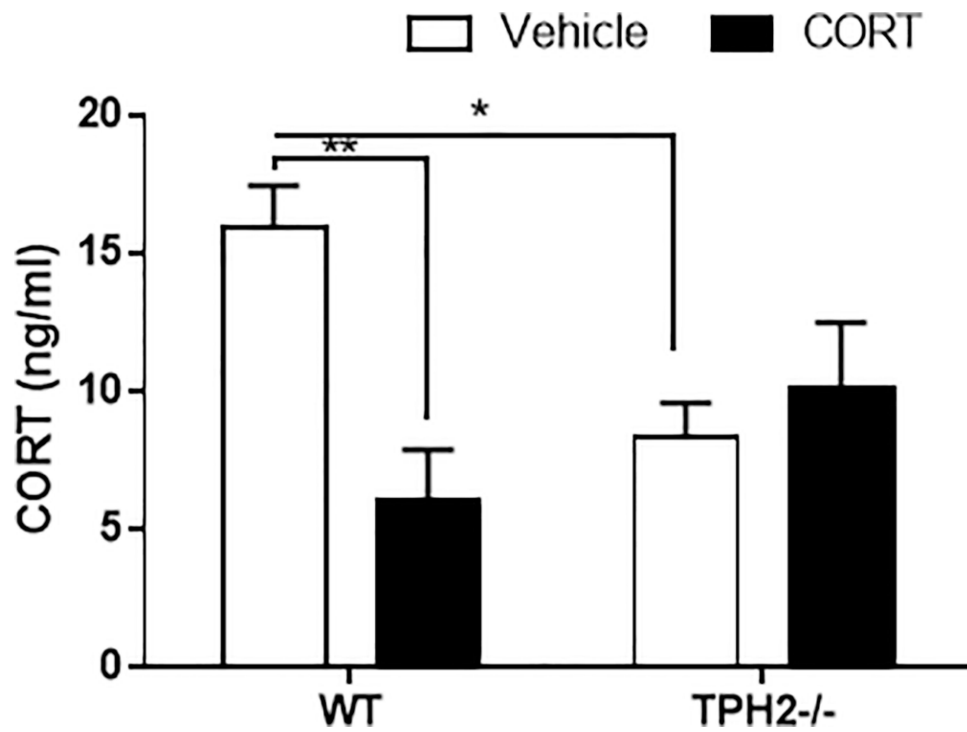
Fig. 2.
Corticosterone (CORT) levels in serum of WT (n = 5–8) and TPH2–/– (n = 5–7) mice.
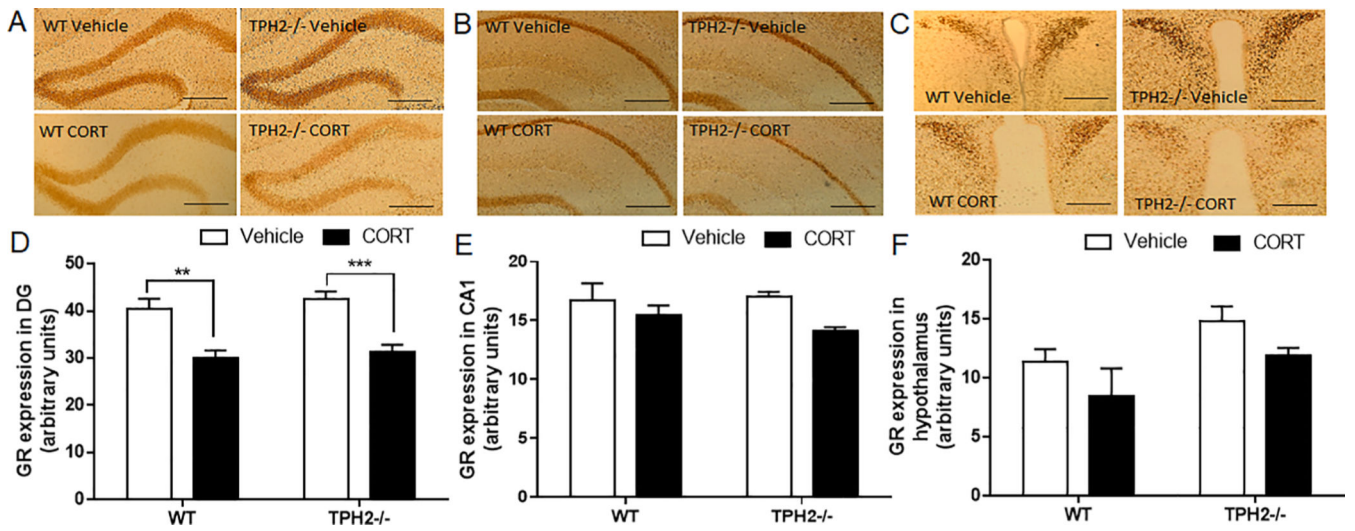Values are mean ± SEM. *p < 0.05, **p < 0.01.

Fig. 3.
Photomicrographs of glucocorticoid receptors (GR) immunoreactivity in the hippocampus dentate gyrus (A), hippocampal CA1 area (B) and hypothalamus (C) of WT (n = 6–7) and TPH2–/– (n = 7–8) mice treated with corticosterone (CORT) or vehicle over 21 days. Expression of GR in the dentate gyrus (D), CA1 area (E) and hypothalamus (F) the subjects mentioned above. Scale bars represent 500 μm. Values are mean ± SEM. **p < 0.01, ***p < 0.001.
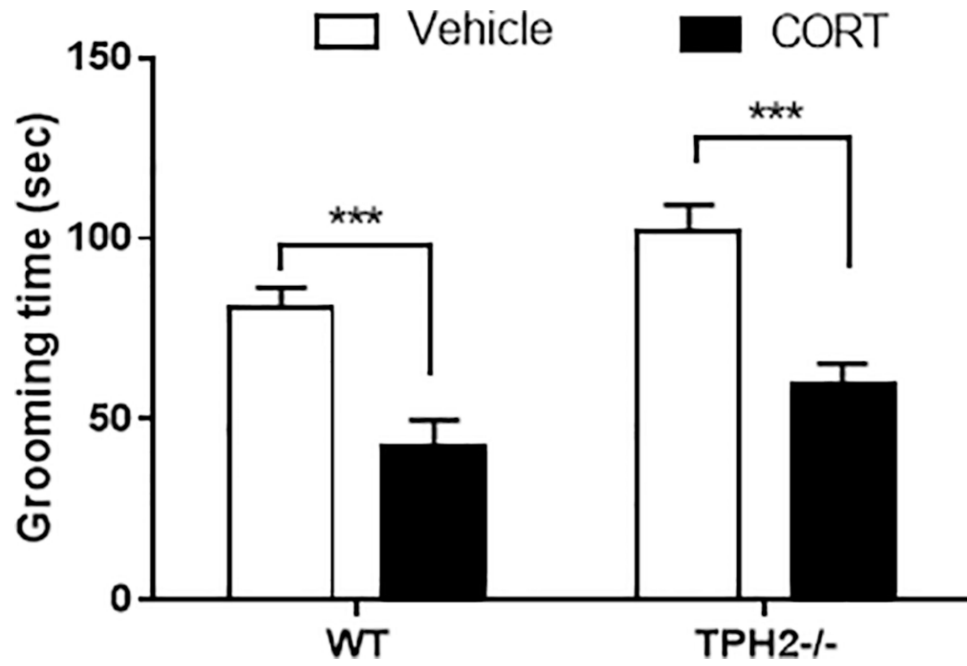
Fig. 4.
Time that WT (n = 9–10) and TPH2–/– (n = 9–10) mice treated with corticosterone (CORT) or vehicle spent grooming in the splash test. Mean ± SEM values. ***p < 0.001.
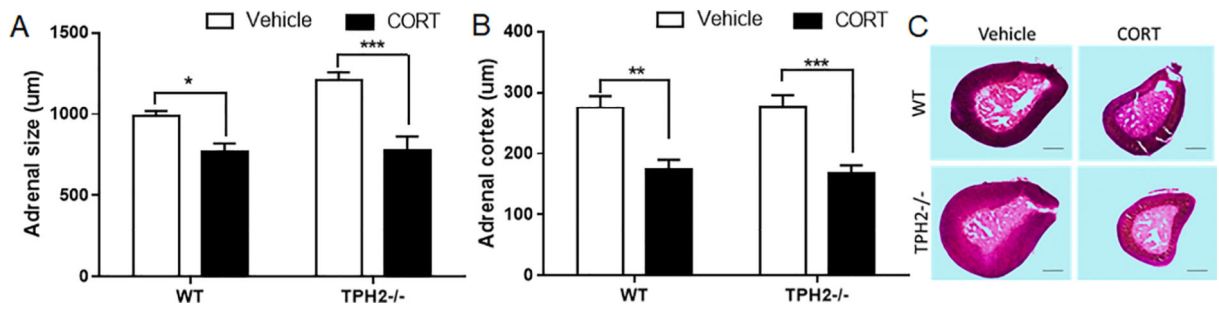
Fig. 5.
Whole adrenal gland size (A), adrenal cortex size (B) and hematoxylin-eosin staining of adrenal glands (C) in WT (n = 7–8) and TPH2–/– (n = 6–7) mice treated with corticosterone (CORT) or vehicle over 21 days. Scale bars represent 250 μm. Values are mean ± SEM. *p < 0.05, **p < 0.01, ***p < 0.001.
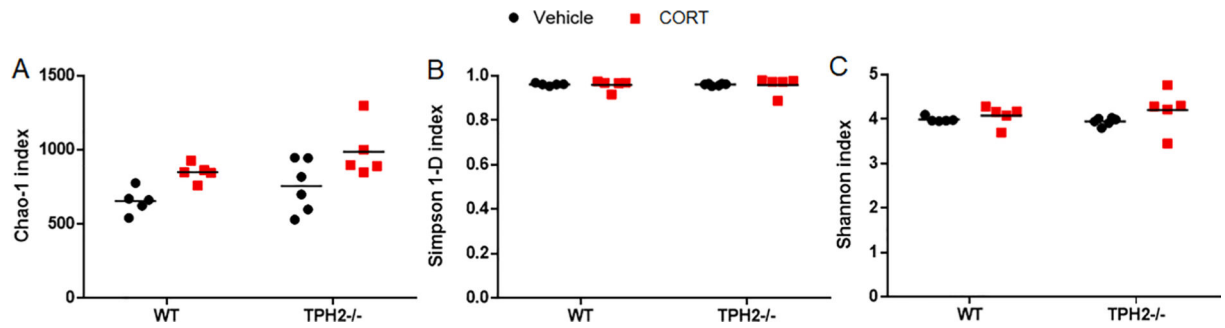
Fig. 6.

Scatter plots of the indices of microbial α-diversity Chao-1 (A), reverse Simpson (B), and Shannon (C) in WT (n = 5–7) and TPH2–/– (n = 6–7) mice treated with corticosterone (CORT) or vehicle over 21 days. Values are mean ± SEM.
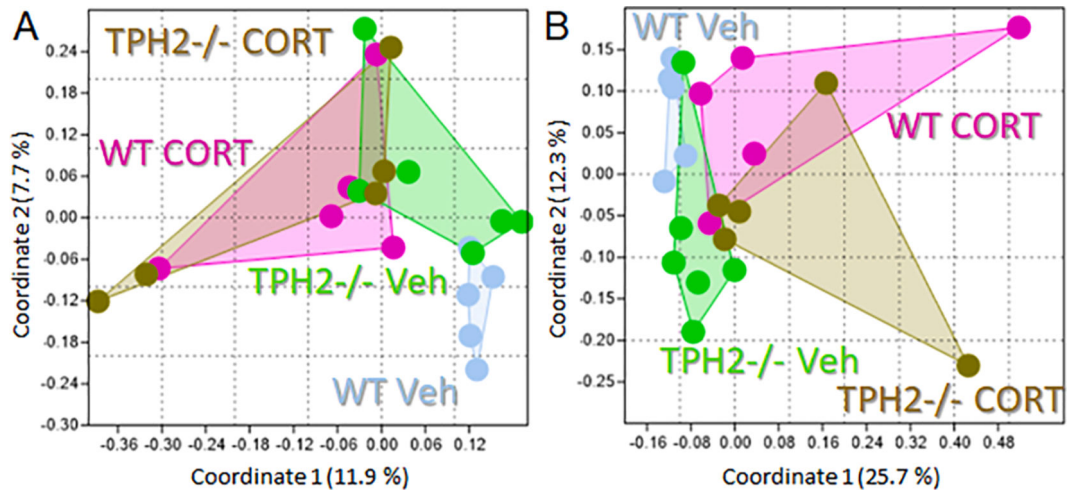
Fig. 7.
Principal coordinate analyses of the microbial β-diversity indices Jaccard (A) and Bray-Curtis (B) in WT (n = 5) and TPH2−/− (n = 5–6) mice treated with corticosterone (CORT) or vehicle (Veh) over 21 days.
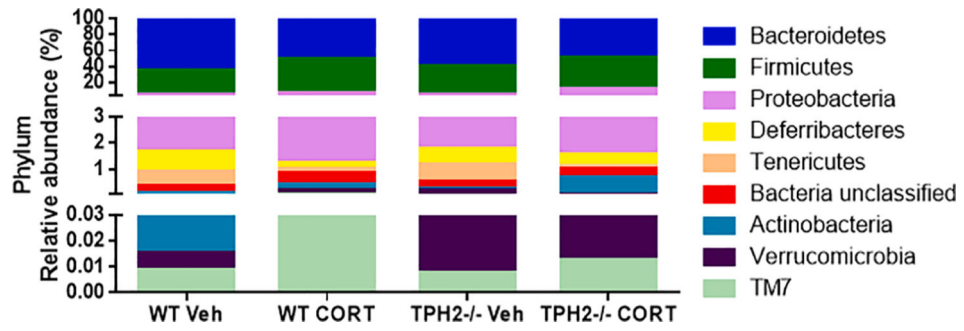
Fig. 8.
Relative abundance (%) of the most prominent bacterial phyla in WT (n = 5) and TPH2−/− (n = 5–6) mice treated with corticosterone (CORT) or vehicle (Veh) over 21 days.
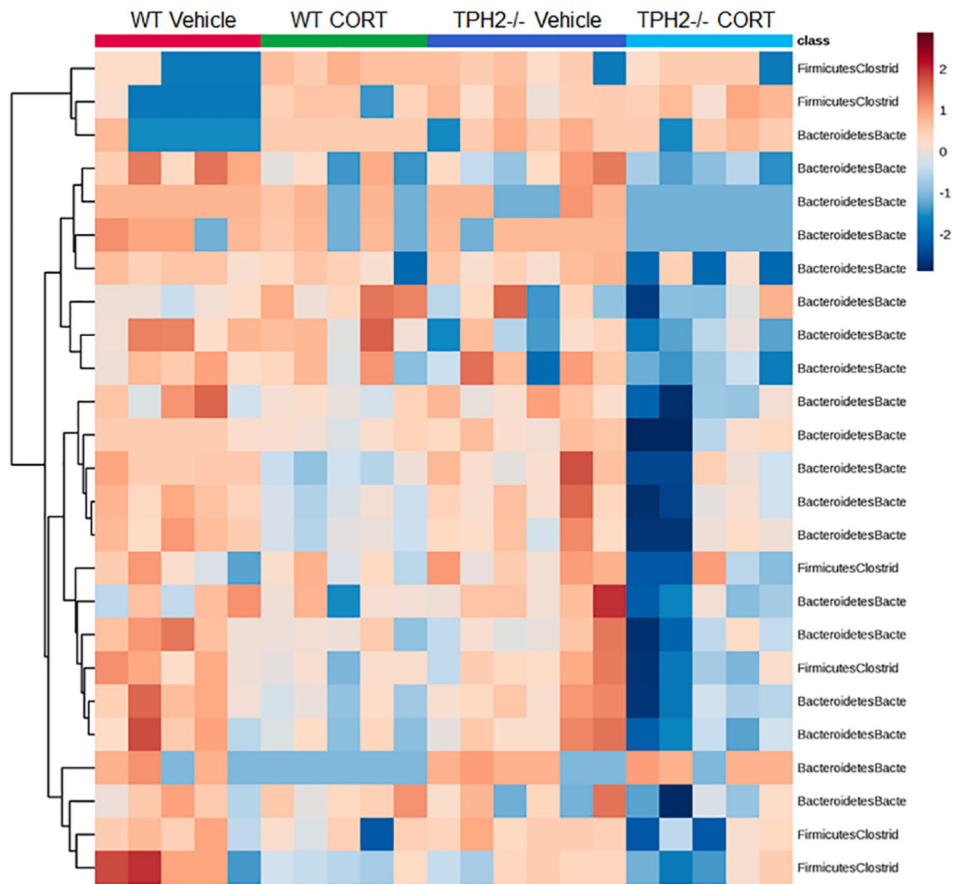
Fig. 9.
Heat map illustrating patterns in the top 25 operational taxonomic units with relative abundance greater than 4% in WT (n = 5) and TPH2−/− (n = 5–6) mice treated with corticosterone (CORT) or vehicle over 21 days. All subjects in each group are arrayed in columns and bacterial taxonomies are indicated in rows. Clustering along the y-axis was done using the Ward algorithm.
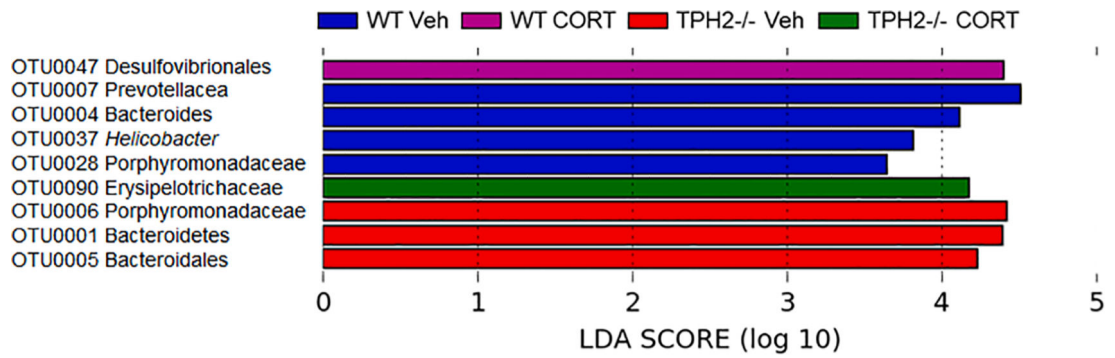
Fig. 10.

Bacterial taxa that were differentially abundant across the WT and TPH2–/– genotypes treated with corticosterone (CORT) or vehicle (Veh). LEfSe was carried out using the Galaxy Project and the results are displayed as bars, the lengths of which are indicative of the linear discriminant analysis score for each operational taxonomic unit (OTU). The taxonomic identity of each OTU is indicated to the left of each bar. All groups are statistically significant compared to each other (LDA > 3.6).

Table 1

OTUs identified by BLAST with a 16S rRNA gene sequence identity 99% to the specified bacterial species across the WT and TPH2– /– genotypes treated with corticosterone or vehicle.

OTU #	Bacteria sp.	Identity (%)	Group
OTU0004	*Bacteroides acidifaciens*	100	WT Vehicle
OTU0037	*Helicobacter hepaticus*	100	WT Vehicle
OTU0072	*Lactobacillus reuteri*	99.6	TPH2–/– Vehicle
OTU0090	*Fecalibaculum rodentium*	99.2	TPH2–/– CORT